3-D Analytical Models for the Short-Channel Effect Parameters in Undoped FinFET Devices

Hamdy Abd El Hamid[*], Jaume Roig[**], Valeria Kilchytska[***], Denis Flandre[***], Benjamin Iñiguez[*]

[*] Departament d'Enginyeria Electrònica, Elèctrica i Automàtica, Universitat Rovira i Virgili, 43007-Tarragona, Spain. E-mail: hamdy.abd@urv.cat, benjamin.iniguez@urv.cat
[**] LAAS / CNRS, 7 avenue du Colonel Roche, 31077 Toulouse Cedex 4, France
[***]Microelectronics Laboratory, Université catholique de Louvain (UCL), Louvain-la-Neuve, B-1348, Belgium

ABSTRACT

An analytical and scalable model for the subthreshold swing and the threshold voltage in FinFETs has been developed by solving the 3-D Poisson equation using appropriate techniques. The model is also based on a physical analysis of the conduction path. The mobile charge term was considered in the 3-D Poisson's equation to be solved. Due to its 3-D basis, the model inherently accounts for short-channel effects, such as the subthreshold swing degradation, threshold voltage roll-off and the Drain Induced Barrier Lowering (DIBL) effect. A very good agreement with 3-D numerical simulations has been obtained.

Keywords: undoped FinFET, 3-D Poisson's equation, conduction path, threshold voltage, threshold voltage roll-off , DIBL

1 INTRODUCTION

The FinFET transistor is one of the most promising multi-gate MOS devices, due to the excellent electrostatic control of the channel by the triple gate (which allows the device to be scaled down to several tens of nanometers of channel length) and to the relative simplicity of its process.
The FinFET performance has been studied from experimental data [1-3] and also through numerical simulations [4]. However, so far very little work has been done on the analytical modeling of FinFET device characteristics, probably due to the fact that, as the devices dimensions are scaled down, the electrostatics of this device becomes fully three- dimensional (3-D); Poisson's equation has to be solved in 3-D and, as a result, the development of an analytical model becomes a difficult problem to solve.

G. Pei, *et. a*l., [5], presented 3-D subthreshold swing and threshold voltage roll-off models, but they are only valid for doped FinFET devices, because the mobile charge term in the 3-D Poisson's equation is neglected; this is not very accurate in the near threshold regime and, in fact, it is equivalent to neglecting the effect of volume inversion on the threshold voltage. However, a threshold voltage model valid for circuit design must include the effect of volume inversion, which has been found to be significant even in doped Double Gate (DG) MOSFETs [6].

In this paper we present FinFET subthreshold swing and threshold voltage models developed from an analytical solution of 3-D Poisson equation which includes the mobile charge term; this analytical solution has been found by using suitable techniques and making a few approximations valid in the subthreshold and near threshold regimes. After properly defining the location of the conduction path in the fin, we obtained very good agreement with 3-D numerical simulations for the threshold voltage roll-off and the DIBL effect for channel lengths down to 30 nm.

2 POTENTIAL MODEL DERIVATION

Fig. 1 shows the FinFET structure considered in this work. The channel is practically undoped (10^{15} cm^{-3}), the n^+ source and drain are highly doped, buried oxide thickness thickness is 150nm, oxide thickness 1.5nm, gate work function 4.5eV.

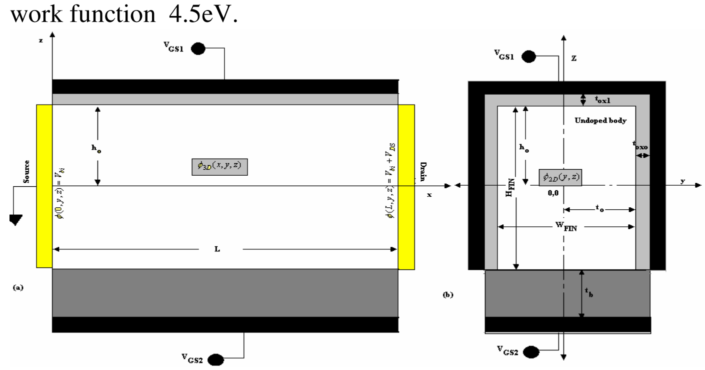

Fig. 1. FinFET Cross section, a) xz- device structure, and b) yz-. device structure

The device electrostatics is governed by the 3-D Poisson's equation:

$$\frac{\partial^2\phi(x,y,z)}{\partial x^2}+\frac{\partial^2\phi(x,y,z)}{\partial y^2}+\frac{\partial^2\phi(x,y,z)}{\partial z^2}=\frac{q}{\varepsilon_{si}}n(x,y,z) \quad (1)$$

where ϕ is the electrostatic potential.
The electron density is given by:

$$n(x,y,z)=n_i e^{[\phi(x,y,z)-\phi_{Fn}(x)]/V_T} \quad (2)$$

where n_i is the intrinsic electron density in silicon, V_T is the thermal voltage, and ϕ_{Fn} is the non-equilibrium quasi-Fermi level referenced to the Fermi level in the source, satisfying the boundary conditions: $\phi_{Fn}(0)=0$, $\phi_{Fn}(L)=V_{ds}$

To solve for the potential in Eq. (1), we have considered that the potential will be the sum of three (the third component included in 2D solution) components as,

$$\phi(x,y,z)=\phi_{2D}(y,z)+\phi_{3D}(x,y,z) \quad (3)$$

Where $\phi_{2D}(y,z)$ is the 2D potential and related to 1D potential as,

$$\phi_{2D}(y,z)=\phi_{1D}(y)+\alpha_o(y)\cdot z+\alpha_1(y)\cdot z^2 \quad (4)$$

with boundary conditions,

$$C_{ox1}\cdot[V_{GS1}-\phi_{ms}-\phi_{2D}(y,z=h_o)]=-\varepsilon_{Si}\left.\frac{\partial\phi_{2D}(y,z)}{\partial z}\right|_{z=h_0} \quad (5)$$

$$C_{ox2}\cdot[V_{GS2}-\phi_{ms}-\phi_{2D}(y,z=-h_o)]=\varepsilon_{Si}\left.\frac{\partial\phi_{2D}(y,z)}{\partial z}\right|_{z=h_0} \quad (6)$$

V_{GS1} is the potential applied on both left/right and top gate. ϕ_{ms} is the gate work function referred to intrinsic silicon, and V_{bi} is the built-in voltage of the source/drain-channel junction

$\phi_{1D}(y)$ is the solution of,

$$\frac{\partial^2\phi(y)}{\partial y^2}=\frac{q}{\varepsilon_{si}}n_i e^{\phi(y)/V_t} \quad (7)$$

with the boundary conditions, $\left.\frac{\partial\phi_{1D}(y)}{\partial y}\right|_{y=0}=0$

$$C_{oxo}\cdot[V_{GS1}-\phi_{ms}-\phi_{1D}(y=t_o)]=-\varepsilon_{si}\cdot\left.\frac{\partial\phi_0}{\partial y}\right|_{y=t_o} \quad (8)$$

We found that:

$$\phi_{1D}(y)=V_T\cdot\ln\left[\frac{B_n^2}{2\cdot\delta}\sec^2(B_n\cdot y)\right] \quad (9)$$

B_n, δ, α_o, and α_1 depend on the technological parameters.

The 3-D potential component is the solution of the remaining 3-D Laplace's equation with boundary conditions,

$$C_{ox1}\cdot[0-\phi_{3D}(x,y,z=h_o)]=-\varepsilon_{Si}\left.\frac{\partial\phi_{3D}(x,y,z)}{\partial z}\right|_{z=h_0} \quad (10)$$

$$C_{ox2}\cdot[0-\phi_{2D}(y,z=-h_o)]=\varepsilon_{Si}\left.\frac{\partial\phi_{3D}(x,y,z)}{\partial z}\right|_{z=h_0} \quad (11)$$

$$\phi_{3D}(0,y,z)\big|=V_{bi}-\phi_{2D}(y,z)$$

$$\phi_{3D}(L,y,z)\big|=V_{DS}+V_{bi}-\phi_{2D}(y,z) \quad (12)$$

The approximations used to obtain the analytical solution were to consider that in (2) ϕ_F is constant along the channel (which is valid in subthreshold) and equal to its value at the source end of the channel, and that the short-channel effects are not very severe [7,8], so that ϕ_{1D} is the dominant potential contribution for the electron charge density in (2).

An analytical expression is obtained

$$\phi_{3D}(x,y,z)=\cos(\lambda_y\cdot y)\cdot\left\{\sum_{N=0}^{1}\begin{matrix}\frac{\Delta P_2}{\Delta R_1}\cos(\lambda_{zN}\cdot z)\cdot[V_{DS}\cdot D_1+V_{bi}\cdot D_o]- \\ \left(\frac{S_1}{\Delta R_1}\cos(\lambda_{zN}\cdot z)+\frac{S_o}{\Delta R_o}\cdot\sin(\lambda_{zN}\cdot z)\right)\cdot D_o\end{matrix}\right\} \quad (13)$$

where

$$D_o=\frac{\sinh(\lambda_x\cdot x)-\sinh[\lambda_x\cdot(x-L)]}{\sinh(\lambda_x\cdot L)} \qquad D_1=\frac{\sinh(\lambda_x\cdot x)}{\sinh(\lambda_x\cdot L)} \quad (14)$$

ΔP_2, ΔR_o, ΔR_1, S_o, and S_1 depend on the technological parameters. λ_y, λ_z, and λ_x are the eigen values, where, $\lambda_x=\sqrt{\lambda_z^2+\lambda_y^2}$

Fig. 2 shows the obtained electrostatic potential along the channel length for different values of the applied voltages.

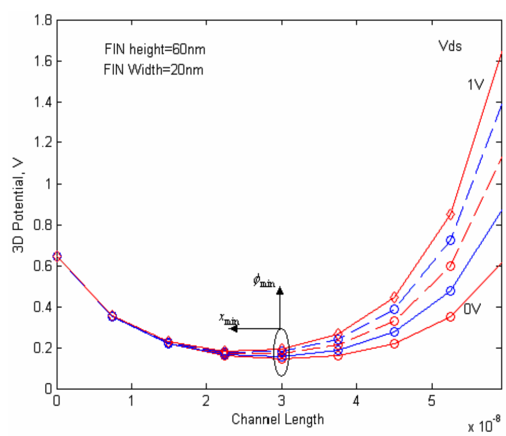

Fig.2 3-D potential distribution along the device channel for different V_{ds}, and V_{GS1}=0.12V, and V_{GS2}=0V

3 SUBTHRESHOLD SWING MODEL

Using the obtained potential distribution over the channel region, we can find the minimum potential point in the channel length direction, known as the "virtual cathode". At this point an energy barrier is formed, over which free electrons diffuse from the source and then are swept into the drain forming the subthreshold drain current.

NSTI-Nanotech 2007, www.nsti.org, ISBN 1420061844 Vol. 3, 2007

We obtain an analytical expression of the location of the virtual cathode, and therefore, of the minimum value ϕ_{min} .

We assume that the subthreshold drain current, I_D, is proportional to the total amount of free electrons diffusing over the virtual cathode. Then, the subthreshold swing, S, is obtained as:

$$S = \frac{\partial V_{GS}}{\partial \log I_D} = \left[\frac{2 \cdot \int_{z=-h_o}^{h_o} \int_{y=0}^{t_o} n_m(y,z) \frac{\partial \phi_{min}(y,z)}{\partial V_{GS}} dydz}{2 \cdot \int_{z=-h_o}^{h_o} \int_{y=0}^{t_o} n_m(y,z) dydz} \right]^{-1} V_T \ln(10) \quad (15)$$

Using the expression we obtained for ϕ_{min} we found the subthreshold swing as,

$$S = \left[1 - \sum_{\lambda_{zo,1}} K_1 \cdot \cos(\lambda_y \cdot y_c) \cdot \cos(\lambda_z \cdot z_c) + K_2 \cdot \cos(\lambda_y \cdot y_c) \cdot \sin(\lambda_z \cdot z_c) \right]^{-1} \cdot V_t \cdot \ln(10) \quad (16)$$

where K_1, and K_2 are scaling factors.

We need to define the values of the coordinates of the conduction path, i.e. y_c, and z_c; the conduction path locations along the y and z axis are strong functions of the device dimensions and the applied voltages. However, we can assume that y_c is close to $W_{fin}/4$ (as in a DG MOSFET), whereas z_c is close to the top interface (due to the maximum electric field value on the buried oxide surface, at $V_{gs2}=0$V). For low V_{ds} value, a value of $y_c \sim W_{fin}/4$ (from the center of the fin width, see Chen et. al., [9]), and a value of $z_c \sim 0.94\%$ of H_{fin} (from the bottom interface) give very good fittings with the 3-D numerical simulations. For high V_{ds} values good fittings are obtained with $y_c \sim 3W_{fin}/10$ (from the center of the fin width) and $z_c \sim 0.99\%$ of H_{fin} (from the bottom interface)

The model in Eq. (16) provides a good agreement with both 3-D numerical simulation and experimental results for different values of fin width, height and channel length, as shown in Fig. 3 and Fig. 4.

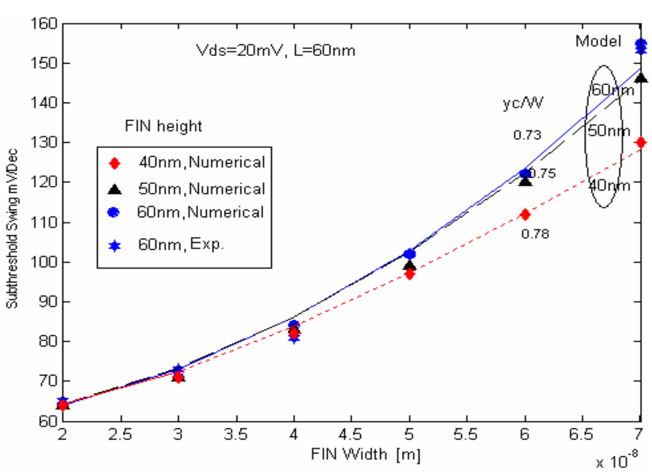

Fig.3 Subthreshold swing for different values of fin height, at a channel length of 60nm.: model (lines), simulations or measurements (symbols)

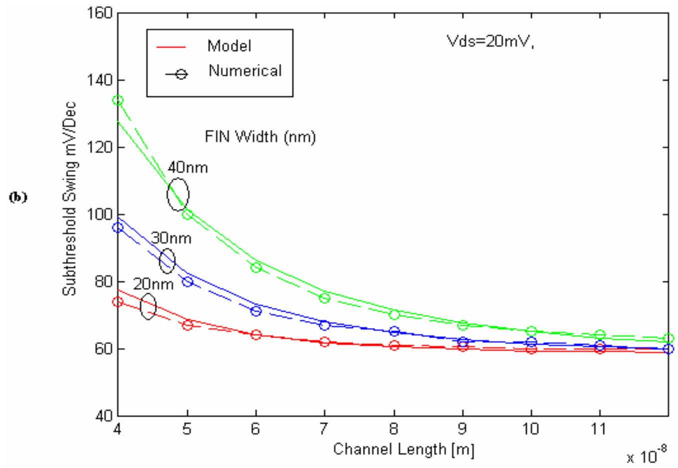

(a)

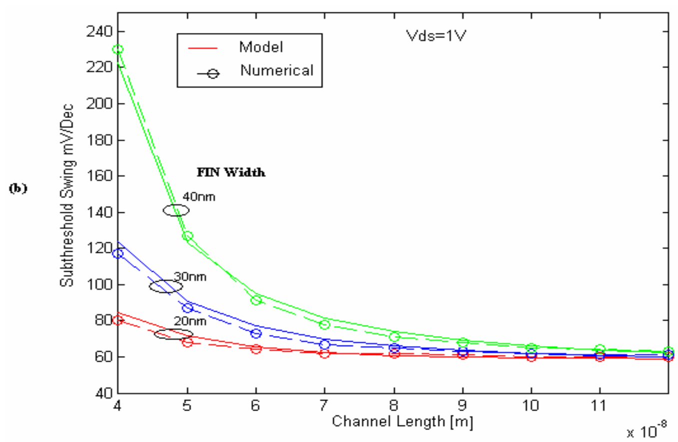

(b)

Fig.3 Subthreshold swing vs. Channel length. H_{FIN}=60nm. Vds=20 mV (a) and 1 V (b).

4 THRESHOLD VOLTAGE MODEL

The channel charge density per unit length can be obtained as,

$$Q_{inv} = 2 \int_{y=0}^{t_o} \int_{z=-h_o}^{h_o} n_i \cdot e^{\frac{\phi_{min}(y,z)}{V_t}} dzdy \quad (17)$$

ϕ_{min}(y,z), is the minimum potential value (virtual cathode),

The last integral in the equation for Q_{inv}, (17), can be solved by assuming that, in every half of the fin, its main contribution takes place at a location equal to $W_{fin}/4$; this is the location of the conduction path along the fin width (considering one half of the fin in the y direction) if we consider the FinFET as a DGMOSFET in which the film thickness is equal to the fin width.

However, the device is asymmetric along z-axis (not only the structure but also the biasing) which will lead to an asymmetric carrier distribution. But we can consider that the result of the integral in (17) is equal to the value of the integrand at the location of the conduction path over an effective height equal to αH_{fin}, where α ($\leq$1) is a correction factor which depends on H_{fin} and W_{fin}, and its value will be extracted numerically.

The inversion charge can written, in terms of α, as,

$$Q_{inv} = n_i \cdot W_{FIN} \cdot (\alpha \cdot H_{FIN}) \cdot e^{\frac{\phi_{min}(y_c, z_c)}{V_t}} \tag{18}$$

$y_c(=W_{FIN}/4)$, and z_c give the location of the conduction path in the *y* and *z* directions,, respectively.

If Q_{TH} is the channel charge density (per unit length) at the threshold condition, from (18) and using the expression of the minimum electrostatic potential, we can calculate the threshold voltage as,

$$V_{TH} = \phi_{ms} + \frac{1}{1 - S_{gs}} \cdot \left(V_t \ln\left(\frac{Q_{TH}}{n_i \cdot W_{FIN} \cdot \alpha \cdot H_{FIN}} \right) - S_{ds} \right) \tag{19}$$

In the FinFET threshold voltage model, the value of α makes it to tend to the DG MOSFET model for very large fin heights and to the square GAA MOSFET model for a symmetric device structure.

We have selected only one value for Q_{TH} from the numerical simulation results of inversion charge characteristic at a very long channel length (and H_{fin}=60nm, and W_{fin}=40nm); by comparing our model in Eq. (18), with the threshold voltage obtained numerically, the value of α is calculated. However, we have found at a comparable W_{fin}/H_{fin} ratio only one value for Q_{TH} will lead to an acceptable threshold voltage with the numerical simulation results for all device dimensions, where the Q_{TH} value is a fraction of (10^{15} m^{-1}).

In devices where the channel is long with respect to the devices height, and thickness, S_{gs} and S_{ds} are close to zero. Therefore, the long channel threshold voltage can be written as:

$$V_{TH} = \phi_{ms} + V_t \ln\left(\frac{Q_{TH}}{n_i \cdot W_{FIN} \cdot \alpha \cdot H_{FIN}} \right) \tag{20}$$

We obtained the threshold voltage roll-off (see Fig.6) as the difference between (19) and (20).

A good agreement has been obtained between model and 3-D numerical simulation results for a broad range of fin widths and fin heights, as shown in Fig. 5.

The DIBL effect can be calculated as the difference between the threshold voltage at high drain-source voltage (1V) and the threshold voltage at very small values (10mV) of drain-source voltage. We have observed very good agreement between the calculated DIBL coefficient and the one obtained numerically has been observed, as shown in Fig. 6.

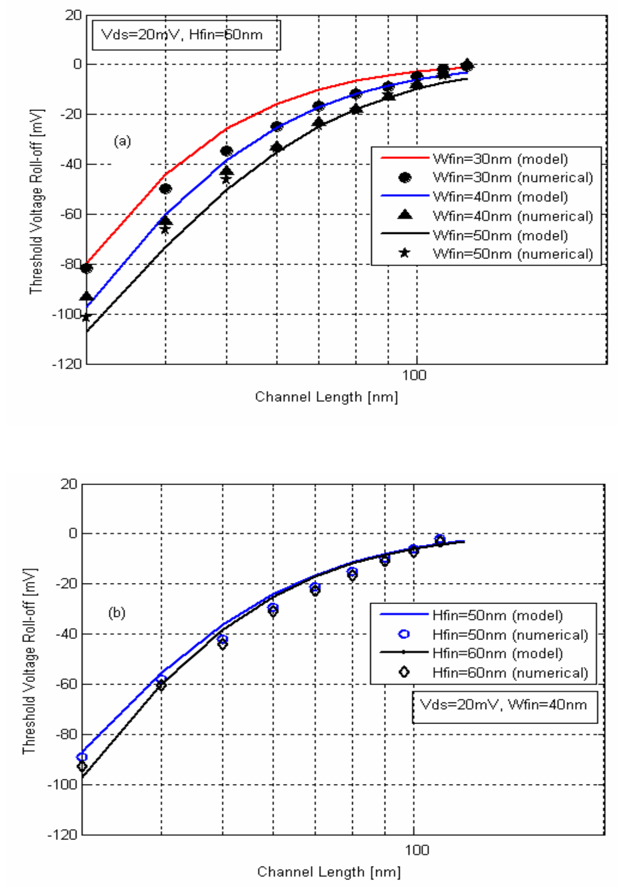

Fig.5 Threshold voltage roll-off vs. channel length for different values of fin widths (a) and fin heights (b).

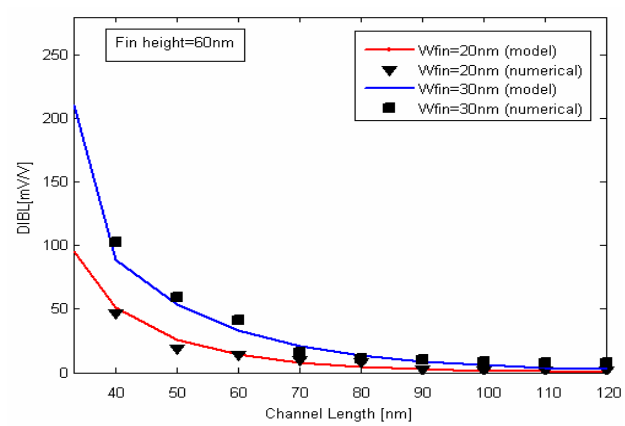

Fig.6 DIBL vs. channel length for different fin widths

NSTI-Nanotech 2007, www.nsti.org, ISBN 1420061844 Vol. 3, 2007

5 CONCLUSIONS

In this paper, after analytically solving the 3-D Poisson's equation for a FinFET, using appropriate techniques, we have developed analytical scalable models of the subthreshold swing and threshold voltage, taking into account the voltage-dependent position of the conduction path. Very good agreement has been obtained with 3-D numerical simulations for the subthreshold swing, threshold voltage, the threshold voltage roll-off, and the DIBL coefficient for channel lengths down to 30 nm.

6 ACKNOWLEDGEMENTS

This work was supported by the European Commission under Contract IST-506844 ("SINANO"), by the Spanish Ministerio de Ciencia y Tecnología under Projects TEC2005-06297/MIC and by the Distinction of the Catalan Government for the Promotion of University Research. The authors wish to thank the IMEC, Leuven, Belgium, in particular Dr. N. Collaert, for providing the experimental devices.

REFERENCES

[1] M. R.Rahman, "Design and Fabrication of Tri-Gated FinFET", *22nd Annual Microelectronic Engineering Conference*, May 2004

[2] D. Hisamoto, et al., "FinFET—A self-aligned double-gate MOSFET scalable to 20 nm," *IEEE Trans.Electron Devices*, vol. 47, pp. 2320-2325, Dec. 2000.

[3] D. Lederer, V. Kilchytska, T. Rudenko, N. Collaert, D. Flandre, A. Dixit, K. De Meyer, and J. P. Raskin, FinFET analogue characterization from DC to 110 GHz, *Solid-State Electronics*, vol. 49, no. 9, pp. 1488-1496, September 2005.

[4] Seung-Hwan Kim, Jerry G. Fossum, and Vishal P. Trivedi, " Bulk Inversion in FinFETs and Implied Insights on Effective Gate Width", *IEEE Trans. on Electron Devices*, vol. 52, no. 9, pp. 1993-1997,September 2005.

[5] G. Pei, J. Kedzierski, P. Oldiges, M. Ieong, and E. C.-C. Kan, " FinFET Design Considerations Based on 3-D Simulation and Analytical Modeling", *IEEE Trans. on Electron Devices*, vol. 49, no. 8, pp. 1411-1419, August 2002

[6] P. Francis, A. Terao, D. Flandre, F. van de Wiele, "Modeling of ultrathin Double-Gate nMOS/SOI Transistors," *IEEE Trans. on Electron Devices*, vol.41, no.5, p.715-720, May 1994,.

[7] H. Abd-Elhamid, B. Iñiguez, D. Jiménez, J. Roig, J. Pallarès, and L. F. Marsal, "Two-Dimensional Analytical Threshold Voltage Roll-Off and Subthreshold Swing Models For Undoped Cylindrical Gate All Around MOSFET," Solid-State Electronics, vol. 50, no. 5, pp. 805-812, May 2006

[8] H. Abd-Elhamid, B. Iñiguez and J. Roig, "Analytical Model of the Threshold Voltage and Subthreshold Swing of Undoped Cylindrical Gate All Around MOSFETs," *IEEE Transaction on Electron Devices*, Vol. 52, no. 3, March 2007

[9] Q. Chen, B. Agrawal and J. D. Meindl, "A Comprehensive Analytical Subthreshold Swing Model for Double-Gate MOSFETs," ," *IEEE Trans. on Electron Devices,* vol. 49, no. 6, pp. 1086-1090, June 2002.